

# Run-Length-Limited ISI-Mitigation (RLIM) Coding for Molecular Communication

Melih Şahin, *Student Member, IEEE*, Ozgur B. Akan, *Fellow, IEEE*

**Abstract**—Inter-symbol interference (ISI) is a significant challenge in diffusion-based communication channels, where residual molecules from previous transmissions interfere with the current signal interval, leading to detection errors. We introduce a new infinite family of coding schemes, which we name RLIM, that require each 1-bit to be followed by at least  $i$  consecutive 0-bits, where  $i$  is any chosen positive integer. This enhances ISI mitigation and improves error correction capabilities compared to existing ISI-mitigating channel codes. Through extensive simulations, we demonstrate that the codebooks derived from the proposed RLIM scheme significantly reduce bit error rate compared to prominent coding methods. Simulation results also reveal that an important constraint in RLIM codes is redundant under zero-drift conditions, removal of which makes them equivalent to run-length-limited (RLL) codes. Notably, despite this equivalence, the proposed family of RLIM coding schemes retains a distinct power optimization constraint and employs a specialized error correction algorithm, preserving its unique character and advantages. Furthermore, in diffusion-based channels with time-varying drift, the previously redundant constraint becomes critical for ensuring robust detection, thus demonstrating the enhanced applicability of proposed RLIM codes for such channels as well.

**Index Terms**—Molecular communication (MC), channel coding, diffusion, run-length-limited (RLL) coding

## I. INTRODUCTION

IN an MC channel, as shown in Fig. 1, a transmitter and a receiver are surrounded by a fluidic environment that facilitates the diffusion-based movement of particles [1], [2]. This diffusive and seemingly-random movement of particles is characterized by Brownian Motion [3], [4]. In this model, the transmitter releases a number of information molecules at the start of each signal interval, which are then detected by the receiver if they come into its vicinity. The receiver decodes the information sent through the channel based on when, how many, and what types of information molecules it absorbed. MC causes a high degree of inter-symbol interference (ISI), a phenomenon where the gradual accumulation of information molecules, not yet absorbed by the receiver, impairs the receiver's ability to correctly decode the intended signal [5].

A number of coding schemes have been used or proposed in the MC literature, including ISI-mitigating codes [6], ISI-free codes [7], Uncoded BCSK [8], and Hamming [9], [10]

Melih Şahin and O. B. Akan are with the Center for neXt-generation Communications (CXC), Department of Electrical and Electronics Engineering, Koç University, Istanbul 34450, Türkiye (e-mail: {melihshahin21, akan}@ku.edu.tr).

O. B. Akan is also with the Internet of Everything (IoE) Group, Department of Engineering, University of Cambridge, Cambridge CB3 0FA, U.K. (e-mail: oba21@cam.ac.uk).

This work was supported in part by the AXA Research Fund (AXA Chair for Internet of Everything at Koç University).

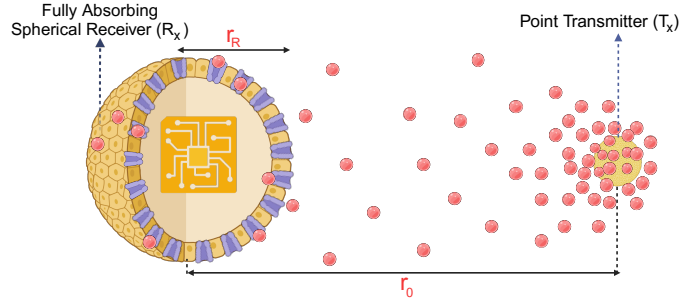


Fig. 1: MC Channel [11]

codes. In terms of bit error rate (BER), ISI-mitigating codes have been shown to outperform these techniques [6]. Through extensive MC simulations across diverse scenarios, we demonstrate that our novel infinite family of coding schemes,  $RLIM_i(n)$  for  $i \in \{2, 3, 4\}$ , offers a significant BER advantage over prominent methods, including ISI-mitigating codes. The key feature of  $RLIM_i(n)$  (where  $n$  represents the code length) is that it ensures the transmission of  $i$  consecutive 0-bits following each 1-bit. This design equips RLIM codes with enhanced error correction capabilities compared to existing MC channel coding schemes.

The structure of this paper is as follows: In the initial part of Section II, system model is provided. Section II-A gives the codebook constructions for the proposed  $RLIM_i(n)$ . Error-correction and detection algorithms are given in Section II-B. An analytical estimation of static threshold is available in Section II-C. In Section III, MC channel simulation results are provided. This paper is concluded in Section IV.

## II. RUN-LENGTH-LIMITED ISI-MITIGATION (RLIM) CODING

One of the most wide-spread MC modulation techniques [12] is the binary concentration shift keying (BCSK) [8]. In BCSK, if a current signal interval corresponds to a 1-bit, a certain number of information molecules are released into the environment from the transmitter at the very start of that signal interval. If a current signal interval corresponds to a 0-bit, no information molecules are released. This paper uses BCSK modulation and assumes perfect time synchronization between the transmitter and receiver, both of which are common approaches in most MC coding studies [1].

The analytical function [13] that gives the probability that an information molecule touches (i.e., gets absorbed by) the

fully absorbing spherical receiver until time  $t$  (in seconds) is

$$F(t) = \frac{r_R}{r_0} \cdot \operatorname{erfc}\left(\frac{r_0 - r_R}{\sqrt{4 \cdot D \cdot t}}\right), \quad (1)$$

where  $r_R$  denotes the radius of the spherical receiver in  $\mu\text{m}$ ,  $r_0$  represents the distance between the center of the spherical receiver and the point transmitter in  $\mu\text{m}$ ,  $D$  is the diffusion coefficient of the fluidic environment in  $\mu\text{m}^2/\text{s}$ , and  $\operatorname{erfc}(\cdot)$  denotes the complementary error function. The  $i^{\text{th}}$  channel coefficient,  $p_i$ , is defined to be the probability that a molecule, emitted in the  $k^{\text{th}}$  signal interval, gets absorbed during the  $(k + i - 1)^{\text{th}}$  signal interval. Channel coefficients [1] are

$$p_i = F(i \cdot t_s) - F((i - 1) \cdot t_s), \quad i = 1, 2, \dots, I, \quad (2)$$

where  $I$  is the channel memory, and  $t_s$  is the signal interval duration. Let  $b_j$  represent the bit information transmitted in the  $(j - 1)^{\text{th}}$  previous signal slot (with  $b_1$  indicating the bit from the current signal interval and  $b_2$  indicating the bit from the previous interval). Through basic probability theory [14], the number of expected molecules,  $N_{exp}$ , to be detected in the current signal interval can then be modeled by using a summation of binomial distribution expressed as

$$N_{exp} \sim \left( \sum_{j=1}^I b_j \cdot \mathcal{B}(M, p_j) \right) + \mathcal{N}(0, \sigma_n^2), \quad (3)$$

where  $M$  is the number of information molecules emitted at the start of each signal interval for the transmission of a 1-bit,  $\mathcal{B}(M, p_j)$  denotes the binomial distribution with  $M$  trials and a success probability of  $p_j$ , and  $\mathcal{N}(0, \sigma_n^2)$  is a Gaussian distribution with mean 0 and variance  $\sigma_n^2$  modelling the counting noise inside the receiver. Using the formula for the mean of a binomial distribution,  $(b_i \cdot M \cdot p_i)$  gives the expected number of molecules released in the  $(i - 1)^{\text{th}}$  previous slot and detected in the current interval. For instance,  $(b_1 \cdot M \cdot p_1)$  is the expected number molecules that are both released and detected in the current signal slot. For sufficiently large values of  $\mathbb{E}(N_{exp})$ , the binomial distribution at (3) can well be approximated by the following Gaussian normal distribution [14]:

$$N_{exp} \sim \mathcal{N}\left(\sum_{j=1}^I b_j \cdot M \cdot p_j, \left(\sum_{j=1}^I b_j \cdot M \cdot p_j \cdot (1 - p_j)\right) + \sigma_n^2\right) \quad (4)$$

Since a summation of binomial distributions can be analytically non-trivial, the normal distribution given in (4) proves to be highly beneficial in many analytical derivations as we demonstrate in Section II-C.

### A. Codebook Derivation

We propose a new infinite family of codebooks, denoted by  $\text{RLIM}_i(n)$ , where  $i, n \in \mathbb{N}$ . Here,  $\text{RLIM}$  stands for run-length-limited ISI-mitigation, with  $i$  representing the order and  $n$  the length. We define the properties of  $\text{RLIM}_i(n)$  as follows.

1. Each 1-bit is followed by  $i$  0-bits, provided  $i$  or more available positions exist following the 1-bit. If fewer than  $i$  positions are available after the 1-bit, all subsequent bits are 0-bits.
2. Each code starts with  $i$  0-bits.
3. Each code must contain at least one 1-bit.

The  $1^{\text{st}}$  and  $2^{\text{nd}}$  restrictions are needed to ensure that, after an accurate detection of a single 1-bit of any code, none of the following  $i$  bits can be a 0-bit. So that, if one of these  $i$  bits are erroneously detected to be a 1-bit, it can be error corrected to a 0-bit. The  $3^{\text{rd}}$  condition has to do with the adaptive-threshold detection technique; and why it is needed will be illustrated in Section II-B. If the  $3^{\text{rd}}$  condition were dropped,  $\text{RLIM}_i(n)$  would be equal to run-length-limited codes of order  $(i, \infty)$  of length  $n$  [15]. Note that, when the order  $i$  of the  $\text{RLIM}$  scheme is set to 1, resultant codes correspond to the ISI-mitigating codes.

Let  $C_i(n)$  denote the subset of all codes belonging to  $\{0, 1\}^n$ , with the  $1^{\text{st}}$  condition in place, but the  $2^{\text{nd}}$  and  $3^{\text{rd}}$  conditions dropped. In coding literature,  $C_i(n)$  is known as a  $d$ -limited sequence (where  $d$  substitutes  $i$ ) [16]. Then, through basic Combinatorics, and from [16],  $C_i(n)$  conforms to the following relation (5), where each row represents a distinct code, and  $|\cdot|$  is the cardinality function. Note that  $\mathbf{0}_n^m$  denotes a matrix of 0s with  $m$  columns and  $n$  rows; and similarly  $\mathbf{1}_n^m$  denotes a matrix of 1s with  $m$  columns and  $n$  rows.

$$C_i(n) = \left[ \begin{array}{c|c} \mathbf{0}_{|C_i(n-1)|}^1 & C_i(n-1) \\ \hline \mathbf{1}_{|C_i(n-1-i)|}^1 & \mathbf{0}_{|C_i(n-1-i)|}^i \mid C_i(n-1-i) \end{array} \right] \quad (5)$$

This recursive relation holds, because the elements of  $C_i(n)$  can be categorized into two groups: those that start with a 0-bit, and those that start with a 1-bit. If a code starts with a 0-bit, the remaining part of it can be any element of  $C_i(n-1)$ . Similarly, if a code starts with a 1-bit, this 1-bit must be followed by  $i$  0-bits, then the remaining part can be any element of  $C_i(n-1-i)$ . To obtain the  $\text{RLIM}_i(n)$ , first we need to enforce the  $2^{\text{nd}}$  condition, which was dropped in the derivation of  $C_i(n)$ . That is,  $i$  0-bits are concatenated to the start of each code of  $C_i(n-i)$ . Then, to enforce the  $3^{\text{rd}}$  condition, we need to remove the code that consist entirely of 0-bits from the matrix. These operations can be done via the matrix given below. Note that the superscript (\*) indicates the removal of the code (i.e., the row) consisting completely of 0-bits.

$$\text{RLIM}_i(n) = \left[ \begin{array}{c|c} \mathbf{0}_{|C_i^*(n-i)|}^i & C_i^*(n-i) \end{array} \right] \quad (6)$$

To better illustrate how these matrices can be utilised, we will now obtain the code space of  $\text{RLIM}_2(6)$  using the matrices given above. We first need the base-cases. Let us give  $C_2(1)$ ,  $C_2(2)$ , and  $C_2(3)$ .

$$C_2(1) = \begin{bmatrix} 0 \\ 1 \end{bmatrix}, \quad C_2(2) = \begin{bmatrix} 0 & 0 \\ 0 & 1 \\ 1 & 0 \end{bmatrix}, \quad C_2(3) = \begin{bmatrix} 0 & 0 & 0 \\ 0 & 0 & 1 \\ 0 & 1 & 0 \\ 1 & 0 & 0 \end{bmatrix} \quad (7)$$

Now we apply the recursion matrix given at (5) to obtain the  $C_2(4)$  as follows.

$$C_2(4) = \begin{bmatrix} 0_4^1 & C_2(3) \\ 1_2^1 & 0_2^2 & C_2(1) \end{bmatrix} = \begin{bmatrix} 0 & 0 & 0 & 0 \\ 0 & 0 & 0 & 1 \\ 0 & 0 & 1 & 0 \\ 0 & 1 & 0 & 0 \\ 1 & 0 & 0 & 0 \\ 1 & 0 & 0 & 1 \end{bmatrix} \quad (8)$$

To obtain  $RLIM_2(6)$  we need to apply the matrix given at (6) to the  $C_2(4)$ . This procedure is as follows.

$$RLIM_2(6) = \begin{bmatrix} 0_5^1 & C_2^*(4) \end{bmatrix} = \begin{bmatrix} 0 & 0 & 0 & 0 & 0 & 1 \\ 0 & 0 & 0 & 0 & 1 & 0 \\ 0 & 0 & 0 & 1 & 0 & 0 \\ 0 & 0 & 1 & 0 & 0 & 0 \\ 0 & 0 & 1 & 0 & 0 & 1 \end{bmatrix} \quad (9)$$

Any  $RLIM_i(n)$  can be obtained using the recursive procedure defined in this section. For a given value of  $i$ , only the base cases,  $C_i(1), \dots, C_i(j), \dots, C_i(i+1)$ , where  $1 \leq j \leq i+1$ , should be pre-computed as in (7). This is a trivial task: Each base-case  $C_i(j)$  has, in total,  $j+1$  codes (i.e., rows). The first code of each  $C_i(j)$  is the 0 vector, and the remaining  $j$  codes have the following property: The  $k^{th}$  code (i.e. row) of  $C_i(j)$ , where  $2 \leq k \leq j+1$ , has a 1-bit in the  $(j+2-k)^{th}$  position, with remaining places all assigned with 0-bits.

Finally, to perform encoding and decoding, after deriving the code space  $RLIM_i(n)$ , a bijective function needs to be created between  $\{0, 1\}^{\lfloor \log_2 |RLIM_i(n)| \rfloor}$  and a subset  $S$  of  $RLIM_i(n)$  with size  $2^{\lfloor \log_2 |RLIM_i(n)| \rfloor}$ , where  $\lfloor \cdot \rfloor$  is the floor function. The subset  $S$  should include codes of  $RLIM_i(n)$  with the fewest number of 1-bits. This criterion is important because it ensures that the coding scheme can utilize a greater number of information molecules for transmitting each 1-bit, thereby reducing the bit error rate.

Let us denote such a subset  $S$  of  $RLIM_i(n)$ , by  $RLIM_i(n, k)$  provided that  $|RLIM_i(n)| \geq 2^k$ . That is,  $S$  a minimal subset with size  $2^k$  of  $RLIM_i(n)$  in term of the total number of 1-bits it contains. Please note that there can be multiple such minimal subsets, in which case one of them can randomly be chosen. After creating the subset  $S$ , we order it by the binary values of its codes to facilitate the binary search algorithm during decoding. Specifically, when converting each code in  $S$  back to its associated element in  $\{0, 1\}^k$ , the binary search enables retrieval in  $\mathcal{O}(k)$  time. The Python implementations of codebook generation, encoding, and decoding algorithms, for any  $RLIM_i(n, k)$ , are given in the Code Availability section.

## B. Detection and Error Correction

Assume that an  $RLIM_i(n)$  coding scheme is used. We will adopt the adaptive threshold detection technique. Let  $m$  be the sequence giving the absorbed number of molecules at each signal interval of a code  $c \in RLIM_i(n)$ . Define  $m^{max} =$

---

### Algorithm 1 Proposed Detection with Static Threshold

---

**Require:** let  $m$  be a sequence of number of absorbed molecules with size  $n$ , let  $\tau_{static}$  be the static threshold, let  $i$  be the order of  $RLIM_i(n)$ .

- 1: let *detected\_bit\_sequence* be a sequence of 0s of size  $n$
- 2: **for**  $j \leftarrow 1$  **to**  $n$  **do**
- 3:   **if**  $m[j] \geq \tau_{static}$  **then** *detected\_bit\_sequence*[ $j$ ] = 1
- 4:   **end if**
- 5: **end for**
- 6: **if** *detected\_bit\_sequence*[ $i+1 : n$ ] is the 0-vector **then**
- 7:   *max\_index* =  $i+1$
- 8:   *max\_value* =  $-1$
- 9:   **for**  $h \leftarrow i+1$  **to**  $n$  **do**
- 10:     **if**  $m[h] > \text{max\_value}$  **then**
- 11:       *max\_value* =  $m[h]$
- 12:       *max\_index* =  $h$
- 13:     **end if**
- 14:   **end for**
- 15:   *detected\_bit\_sequence*[*max\_index*] = 1
- 16: **end if**
- 17: **return** *detected\_bit\_sequence*

---

$max(m)$  [6] and  $m_{min} = non\_zero\_min(m)$  [17]<sup>1</sup>. If  $m$  is the 0 vector,  $m_{min}$  is taken to be  $\infty$  (so that  $m$  can be detected as the 0 vector) [17]. Then the adaptive threshold,  $\tau_{adapt}^m$ , pertaining to  $m$  is found as

$$\tau_{adapt}^m = a \cdot m_{min} + (1 - a) \cdot m_{max}, \quad (10)$$

where  $a$  is the channel-specific scaling constant [6]. Note that  $0 \leq a \leq 1$ , and thus  $m_{min} \leq \tau_{adapt}^m \leq m_{max}$ . If the number of absorbed molecules falls below  $\tau_{adapt}^m$ , the corresponding signal interval is detected as a 0-bit, otherwise it is detected as a 1-bit. To find the optimal value of  $a$ , ensuing pilot signals, whose content is pre-known by the receiver, are sent [6]; and the value of  $a$  that results in the least BER value is chosen. The receiver can do this selection by increasing  $a$  from 0 to 1 with a pre-determined step size of  $k$ , whose value, in this paper, is taken to be 0.005. Through this approach, an element of  $m$  that has the value  $m_{max}$  is always detected to be a 1-bit. This is why  $RLIM_i(n)$  needs at least one 1-bit in each code.

Additionally, we provide the implementation of  $RLIM_i$ -specific static-threshold detection technique in Algorithm 1, as we will evaluate both the static and dynamic approaches in Section III. Algorithm 1 strengthens the classical static threshold algorithm [8] by providing robustness against edge cases through its Lines 6–16. It ensures that each detected code contains at least one 1-bit, which holds true for all  $RLIM_i(n)$  codes. Using pilot signals, the optimal static threshold for a given channel can be determined similarly to the optimal scaling constant derivation: By testing thresholds from 1 to  $M$ , the threshold that yields the lowest BER is identified.

<sup>1</sup>For ISI-mitigating codes,  $m_{min}$  is defined as the minimum of  $m - \{m_1\}$  (i.e., the sequence  $m$  excluding its first element). By redefining  $m_{min} = non\_zero\_min(m)$ , this approach is generalized beyond ISI-mitigating codes in [17]. To ensure fairness, we also conducted simulations for ISI-mitigating codes, using its original detection approach, whose results are given in Figs. 4 and 5.

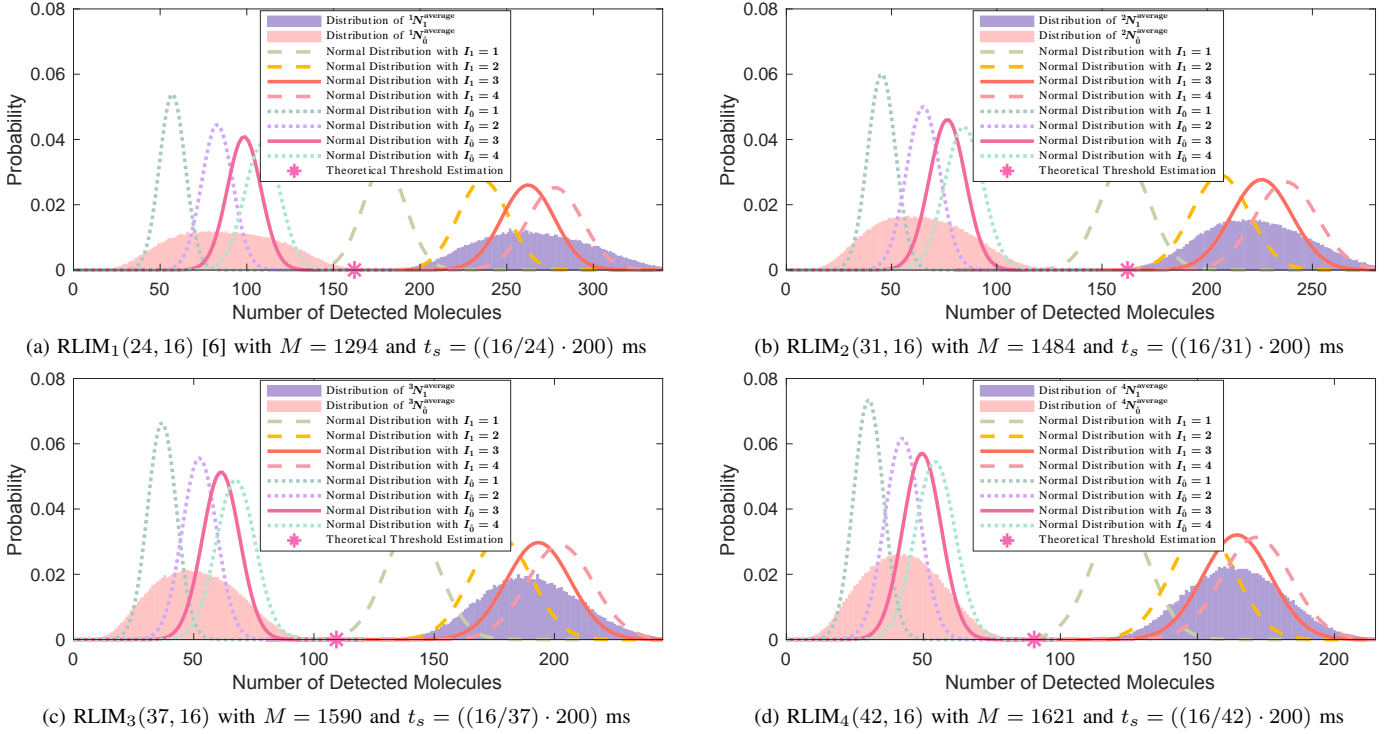


Fig. 2: Detected Molecule Distributions for coding schemes  $RLIM_i(n, 16)$  in an MC channel with,  $D = 79.4 \mu\text{m}^2/\text{s}$ ,  $r_R = 5 \mu\text{m}$ ,  $r_0 = 10 \mu\text{m}$ ,  $I = 200$ ,  $\sigma_n^2 = 0$ , and unnormalized signal interval and molecule counts of  $t_s = 200$  ms, and  $M = 1000$

---

### Algorithm 2 Proposed Error Correction for RLIM

---

**Require:** *detected\_code* with size  $n$ , order  $i$  of  $RLIM_i(n)$

```

1: for  $j \leftarrow 1$  to  $i$  do
2:    $detected\_code[j] = 0$ 
3: end for
4: for  $j \leftarrow 1 + i$  to  $n$  do
5:   if  $detected\_code[j] == 1$  then
6:     for  $h \leftarrow 1$  to  $\min(i, n - j)$  do
7:        $detected\_code[j + h] = 0$ 
8:     end for
9:   end if
10: end for

```

---

By observing that in any code of  $RLIM_i(n)$ , the first  $i$  bits are 0 and no 1-bit can be followed by another 1-bit within the next  $i$  positions, we propose Algorithm 2 for error correction. Note that, when the order  $i$  is set to 1 in Algorithm 2 the resulting algorithm coincides with the one for ISI-mitigating codes presented in [6]. After applying the error correction algorithm to a detected code, the resultant code  $c$  may not be an element of  $RLIM_i(n, k)$ , in which case we iteratively substitute the right-most 1-bit of the code  $c$  with a 0-bit, while searching it inside  $RLIM_i(n, k)$  at each substitution.

### C. Analytical Estimation of Static Threshold

Both the adaptive and static threshold techniques described in the previous section requires sending pilot signals at the start of the communication. However, if the receiver has

the knowledge of the channel parameters, transmitting pilot signals beforehand may no longer be necessary.

Our contribution in this subsection is adapting the analytical derivation method for ISI-mitigating codes to  $RLIM_i(n)$ , with significant modifications which will be clarified at the end of this subsection. Define  $ISI_j = \mathcal{N}(M \cdot p_j, M \cdot p_j \cdot (1 - p_j))$  as per equation (4), which approximates the distribution of the expected number of molecules detected from the emission of  $M$  molecules at the  $(j - 1)^{th}$  previous signal slot. Assuming  $RLIM_i(n)$  is used, when a 1-bit is transmitted in the current signal slot, the distribution of the maximum expected number of detected molecules can be given by the following equation (11).

$${}^i N_1^{max} = \lim_{I_1 \rightarrow \infty} \left( \sum_{k=1}^{I_1} ISI_{1+(i+1) \cdot (k-1)} \right) + \mathcal{N}(0, \sigma_n^2) \quad (11)$$

Rather than deriving a distribution for the maximum possible number of detected molecules, we aim to derive a distribution for the average case. To approximate mean value of a such a distribution,  $I_1$  should be a positive integer. To illustrate this phenomenon, consider the detection count distribution from a binomial simulation of 10000 consecutive codewords, each encoding a random bit sequence of length 16. The simulation uses RLIM codes of orders from 1 to 4 in an MC channel whose simulation parameters are provided in the caption of Fig 2. with corresponding normalized parameters given in the sub-captions. The simulator selection and normalization procedure will be explained in the next section. As can be seen in the right sections of each subfigure in Fig. 2,  $I_1 = 3$  provides a more accurate representation of the molecule count

distribution of 1-bits (shown in purple) compared to other values of  $I_1$ , based on its similarity to the mean value of the distribution. Please note that we observed a similar phenomena for molecule count ( $M$ ) values smaller than 1000. Accordingly, we assume the following approximation in (12):

$${}^i N_1^{average} \approx \left( \sum_{k=1}^3 ISI_{1+(i+1)\cdot(k-1)} \right) + \mathcal{N}(0, \sigma_n^2) \quad (12)$$

Now, consider the case where the current signal slot corresponds to a 0-bit, and all preceding signal slots have been detected accurately. For any code of  $RLIM_i(n)$ , this implies that if there are any 1-bits within  $i$  previous signal slots or if the current interval corresponds to one of the first  $i$  positions of a code, then regardless of the threshold value, the error correction algorithm will always correctly detect the current signal slot as a 0-bit. Accordingly, we denote a 0-bit, which is neither in one of the first  $i$  positions of a code nor has any preceding 1-bits within  $i$  slots, as a  $\hat{0}$ -bit. For the transmission of a  $\hat{0}$ -bit, the maximum expected number of detected molecules is given by the following distribution:

$${}^i N_0^{max} = \lim_{I_0 \rightarrow \infty} \left( \sum_{k=1}^{I_0} ISI_{1+(i+1)\cdot(k)} \right) + \mathcal{N}(0, \sigma_n^2) \quad (13)$$

Setting  $I_0 = 2$  provides a better approximation for the mean of  ${}^i N_0^{average}$  (as shown in the left sections of the subfigures in Fig. 2), but, like other values of  $I_0$ , it fails to accurately model the variance. Moreover,  $I_0 = 2$  is insufficient for predicting the distribution of  ${}^i N_0^{average}$  at higher molecule counts. We chose  $I_0 = 3$ , as given in Eq. (14), as it more accurately approximates the distribution at higher molecule counts.

$${}^i N_0^{average} \approx \left( \sum_{k=1}^3 ISI_{1+(i+1)\cdot(k)} \right) + \mathcal{N}(0, \sigma_n^2) \quad (14)$$

Future research should focus on developing more accurate theoretical distributions for  ${}^i N_1^{average}$  and  ${}^i N_0^{average}$ . While the complex and recursive nature of  $RLIM_i(n, k)$  makes theoretically obtaining these distributions a challenging task, achieving more precise distributions will lead to BER-wise improved static threshold values, which will further discard the need to send pilot signals in advance of the communication.

Let  $P_1$  denote the appearance probability of 1-bits in the code space  $RLIM_i(n, k)$ , and similarly let  $P_0$  denote the appearance probability of  $\hat{0}$ -bits inside the code space  $RLIM_i(n, k)$ . Then, using the Formulae (12) and (14), the probability of correctly detecting the current signal slot, assuming all preceding slots have been detected accurately, is given as

$$P = P_0 \cdot \left[ 1 - Q \left( \frac{\tau_{static} - (\sum_{k=1}^3 M \cdot (p_{1+(i+1)\cdot(k)}))}{\sqrt{(\sum_{k=1}^3 M \cdot (p_{1+(i+1)\cdot(k)}) \cdot (1 - p_{1+(i+1)\cdot(k)})) + \sigma_n^2}} \right) \right] + P_1 \cdot Q \left( \frac{\tau_{static} - (\sum_{k=1}^3 M \cdot p_{1+(i+1)\cdot(k-1)})}{\sqrt{(\sum_{k=1}^3 M \cdot (p_{1+(i+1)\cdot(k-1)}) \cdot (1 - p_{1+(i+1)\cdot(k-1)})) + \sigma_n^2}} \right) \quad (15)$$

where  $Q$  is the tail probability function of the Gaussian normal distribution (i.e.,  $Q(\frac{x-a}{\sqrt{b}})$  gives the integration of  $\mathcal{N}(a, b)$  from  $x$  to  $\infty$ ), and  $\tau_{static}$  is the static threshold constant. We need to find the highest value of (15) in terms of  $\tau_{static}$ . For simplicity, we make the following substitutions:

$$\begin{aligned} A &= (\sum_{k=1}^3 M \cdot (p_{(i+1)\cdot(k)})) \\ B &= (\sum_{k=1}^3 M \cdot (p_{(i+1)\cdot(k)}) \cdot (1 - p_{(i+1)\cdot(k)})) + \sigma_n^2 \\ C &= (\sum_{k=1}^3 M \cdot p_{1+(i+1)\cdot(k-1)}) \\ D &= (\sum_{k=1}^3 M \cdot (p_{1+(i+1)\cdot(k-1)}) \cdot (1 - p_{1+(i+1)\cdot(k-1)})) + \sigma_n^2 \end{aligned} \quad (16)$$

Then, taking the derivative of (15) with respect to  $\tau_{static}$ , and equating it to zero, the analytical derivation of  $\tau_{static}$  is obtained as follows:

$$\tau_{static} = \frac{-B \cdot C + D \cdot A - \sqrt{B \cdot D \cdot ((C-A)^2 - 2 \cdot (B-D) \cdot \log_e \left( \frac{\sqrt{D} \cdot P_0}{\sqrt{B} \cdot P_1} \right))}}{B-D} \quad (17)$$

As an example, for  $RLIM_4(41, 16)^2$ , the values of  $P_0$  and  $P_1$  are  $\frac{996497}{41 \cdot 2^{16}}$  and  $\frac{323397}{41 \cdot 2^{16}}$ , respectively. Then, we calculate the corresponding  $\{p_x\}$  values from equation (2) based on the normalized channel parameters outlined in the sub-caption of Fig. 2(d) and the remaining parameters that are given in the main caption of Fig. 2. Substituting all these values into equation (17) yields a static threshold estimate of 90.4385, as marked in Fig. 2(d).

In [6], the dynamic threshold formula ( $a \cdot m_{min} + (1 - a) \cdot m_{max}$ ) is used in place of  $\tau_{static}$  within equation (15). The values of  $I_1$  and  $I_0$  are both set to 1. The derivative of equation (15) is then taken with respect to  $a$ , set equal to zero, and solved for  $a$ . As a result, in [6], a new analytical value for  $a$  is determined for each detected codeword molecule count sequence,  $m$ , based on  $m_{max}$  and  $m_{min}$ . The dynamic threshold,  $\tau_{dynamic}^m$ , is updated accordingly, as per Eq. (10).

However, in such an analytical approach, regardless of the values  $m_{max}$  and  $m_{min}$  take,  $\tau_{dynamic}^m$  always equals to  $\tau_{static}$ . Therefore, while our approach in this paper for  $RLIM_1(n)$  is equivalent to that in [6] for ISI-mitigating codes when  $I_0 = 1$  and  $I_1 = 1$ , it is computationally more efficient: Our method requires computation only once and can be applied across all codeword detections. Moreover, as demonstrated in Fig. 2, the values  $I_1 = 3$  and  $I_0 = 3$  generally provide a better estimate than  $I_1 = 1$  and  $I_0 = 1$ . This is because, if  $I_1 = 1$  and  $I_0 = 1$  were used, the threshold value would decrease in all four subfigures of Fig. 2; it is evident that this would result in a poorer estimate, as the threshold would intersect with the distribution of  $\hat{0}$ -bits, leading to a greater number of detection errors.

### III. PERFORMANCE EVALUATION

There are 3 main approaches to simulate an MC channel. The first is a discrete particle-tracking-based simulator. This method operates in discrete time steps ( $\Delta t$ ), updating the 3D positions of all information molecules by independently drawing each coordinate from the normal distribution

$$\mathcal{N}(0, 2D\Delta t), \quad (18)$$

<sup>2</sup>As detailed in Section II-A, there may exist multiple  $RLIM_4(42, 16)$  codebooks, each with identical  $P_1$  but slightly different  $P_0$  values. The codebook we used was generated via our custom Python implementation, accessible in the Code Availability section.

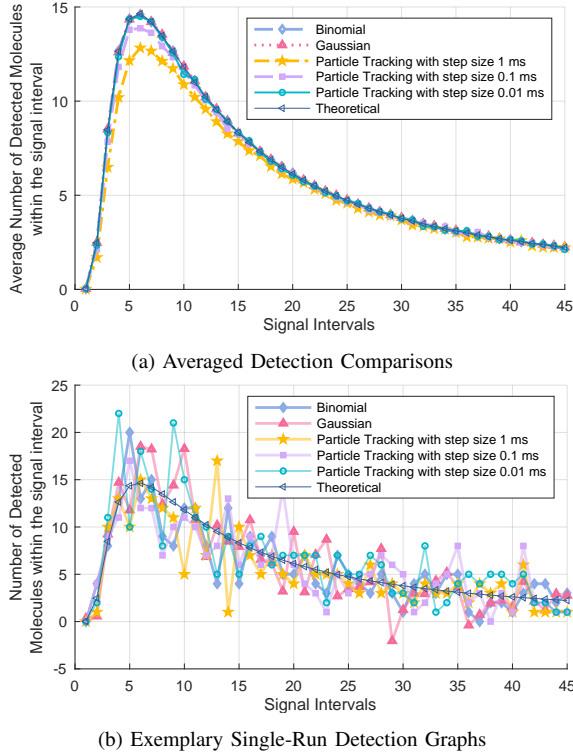


Fig. 3: Simulator Comparisons for Channel Parameters of  $M = 1000$ ,  $D = 79.4 \mu\text{m}^2/\text{s}$ ,  $r_R = 5 \mu\text{m}$ ,  $r_0 = 10 \mu\text{m}$ , and  $t_s = 10 \text{ms}$ .

derived from diffusion physics [18], [19]. It then counts how many molecules are absorbed by the receiver during each time step and removes the absorbed molecules from the simulation. The second approach is to use the summation of binomial distributions expressed in equation (3) to compute the absorbed (i.e., detected) molecule count within a signal interval. The third and computationally fastest approach utilizes the normal distribution formula given in equation (4). Although this method is efficient, it may introduce slight errors for lower molecule counts and can occasionally produce negative detection counts.

To highlight the distinctions between these three approaches, we calculated the averaged number of detected molecules during each signal interval over  $10^4$  samples, as illustrated in Fig. 3(a). These simulations are based on an initial release of 1000 molecules at the start of the first signal interval. The corresponding channel parameters are provided in the caption of Fig. 3. Additionally, Fig. 3(b) presents a graph of individual simulation runs to provide a clearer conceptual illustration. As shown in Fig. 3(a), smaller time steps yield more accurate results in particle-tracking simulations. However, reducing the time step below 1 ms results in excessively longer simulation run-times. In this paper, we employ the binomial distribution approach to simulate the MC channel for its accuracy and computational efficiency.

#### A. Normalizations and Simulation Parameters

To fairly compare different coding strategies, it is essential to normalize the signal interval and the molecule count per

TABLE I: Normalized Signal Interval Values

Coding Method	Signal Interval of	
	200 ms	250 ms
Uncoded [16→16]	200 ms	250 ms
RLIM <sub>1</sub> (24, 16) [16→24] [6]	$(16/24) \cdot 200 \text{ ms}$	$(16/24) \cdot 250 \text{ ms}$
RLIM <sub>2</sub> (31, 16) [16→31]	$(16/31) \cdot 200 \text{ ms}$	$(16/31) \cdot 250 \text{ ms}$
RLIM <sub>3</sub> (37, 16) [16→37]	$(16/37) \cdot 200 \text{ ms}$	$(16/37) \cdot 250 \text{ ms}$
RLIM <sub>4</sub> (42, 16) [16→42]	$(16/42) \cdot 200 \text{ ms}$	$(16/42) \cdot 250 \text{ ms}$
Hamming(4,7) [16→28] [9]	$(16/28) \cdot 200 \text{ ms}$	$(16/28) \cdot 250 \text{ ms}$
ISI-Free(4,2,1) [16→32] [7]	$(16/32) \cdot 200 \text{ ms}$	$(16/32) \cdot 250 \text{ ms}$

TABLE II: Number of 1-bits and Normalized Molecule Counts

Coding Method	Number of 1-bits	Molecule Count ( $M \in \mathbb{N}^+$ )
Uncoded [16→16]	$16 \cdot 2^{15} = 524288$	$1 \cdot M$
RLIM <sub>1</sub> (24, 16) [16→24] [6]	405251	$\lceil 1.2937 \cdot M \rceil$
RLIM <sub>2</sub> (31, 16) [16→31]	353228	$\lceil 1.4842 \cdot M \rceil$
RLIM <sub>3</sub> (37, 16) [16→37]	329724	$\lceil 1.5900 \cdot M \rceil$
RLIM <sub>4</sub> (42, 16) [16→42]	323397	$\lceil 1.6211 \cdot M \rceil$
Hamming(4,7) [16→28] [9]	917504	$\lceil 0.5714 \cdot M \rceil$
ISI-Free(4,2,1) [16→32] [7]	1048576	$\lceil 0.5 \cdot M \rceil$

transmission of a 1-bit values. This ensures that the same amount of information is transmitted across different coding schemes within equal time periods and using an identical number of information molecules. The normalization, as given in [17] and [20], is done as follows: Let  $I$  be the set of all available information. Assume each element of  $I$  are equally likely to be transmitted. Suppose that a coding scheme  $C_1$  encodes all the information of  $I$ , using  $S_1$  bits, and  $M_1$  1-bits. Also assume that a coding scheme  $C_2$  encodes all the information of  $A$ , using  $S_2$  bits, and  $M_2$  1-bits. The signal interval value for coding scheme  $C_2$  should be  $S_1/S_2$  times that of the coding scheme  $C_1$ . Likewise, the number of molecules transmitted per 1-bit in coding scheme  $C_2$  should be  $M_1/M_2$  times that in coding scheme  $C_1$ . For our simulation, let  $I$  be the set  $\{0, 1\}^{16}$ . To encode  $I$  using RLIM <sub>$i$</sub> ( $n$ ) we derive the following inequalities:

$$|\text{RLIM}_1(23)| < 2^{16} < |\text{RLIM}_1(24)| = 75024 < 2^{17} \quad (19)$$

$$|\text{RLIM}_2(30)| < 2^{16} < |\text{RLIM}_2(31)| = 85625 < 2^{17} \quad (20)$$

$$|\text{RLIM}_3(36)| < 2^{16} < |\text{RLIM}_3(37)| = 82628 < 2^{17} \quad (21)$$

$$|\text{RLIM}_4(41)| < 2^{16} < |\text{RLIM}_4(42)| = 67984 < 2^{17} \quad (22)$$

Thus, each of the sets RLIM<sub>1</sub>(24, 16), RLIM<sub>2</sub>(31, 16), RLIM<sub>3</sub>(37, 16), and RLIM<sub>4</sub>(42, 16) are valid codebooks for encoding the information set  $\{0, 1\}^{16}$ . As explained in Section II-A, these codebooks are created in a way that minimizes the total number of 1-bits contained inside them. The normalized signal interval periods are given in Table II, for two different

TABLE III: Simulation Parameters

Parameter	Value
Diffusion coefficient ( $D$ )	$79.4 \mu\text{m}^2/\text{s}$
Distance between $T_x$ and $R_x$ ( $r_0$ )	$9.5 - 11.5 \mu\text{m}$
Receiver radius ( $r_R$ )	$5 \mu\text{m}$
Molecule count per a 1-bit for Uncoded ( $M$ )	$100 - 1000$
Signal interval for Uncoded ( $t_s$ )	$200 - 250 \text{ ms}$
Receiver Gaussian counting noise variance ( $\sigma_n^2$ )	$0 - 20$
Channel Memory ( $I$ )	$200$

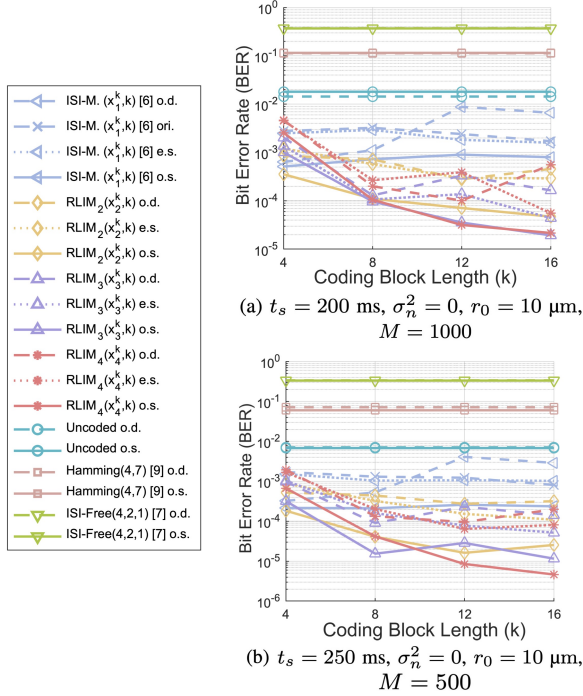


Fig. 4: MC Simulation Results for Different Block Lengths

values: 200 ms and 250 ms. Table I presents the number of 1-bits in RLIM codebooks, along with the molecule count per a transmission of 1-bit values, normalized according to the Uncoded case, where  $\lceil \cdot \rceil$  rounds the given number to the nearest integer. The full range of the parameters used in our comparative MC simulations are listed in Table III<sup>3</sup>.

<sup>3</sup>The values of the parameters  $D$ ,  $r_R$ , and  $r_0$  (with  $r_0 = 10$   $\mu$ m) in Table I are standard in MC literature. They model an MC channel where human insulin hormone is utilised as information molecules [21].

TABLE IV: Values of  $\{x_i^k\}$  in Fig. 4(a) and (b)

$k$	$x_1^k$	$x_2^k$	$x_3^k$	$x_4^k$
4	7	9	11	13
8	13	16	20	23
12	18	24	28	33
16	24	31	37	42

To determine the optimal static threshold and scaling constant<sup>4</sup> values for each coding scheme across different channel parameters, we transmitted a total of 61440 bits by encoding 8 different randomly chosen 7680-bits sequences. Each of the 8 runs was independent. For instance, RLIM<sub>1</sub>(24, 16) encodes 7680 bits using 11520 bits, where all of the bits are transmitted in a contiguous manner. In MC simulations, imitating ISI, which stem from the accumulation of molecules over time, is important. Thus, uninterruptedly simulating long contiguous codewords with a high value of channel capacity (which we took as 200) provides a realistic representation of the MC channel, as we do here.

After having determined the optimal values of the static threshold and scaling constants (along with *min* and optimal *spacing* values for Uncoded, ISI-free, and Hamming schemes<sup>4</sup>), we sent a total of 1290240 bits (8 contiguous runs of the encodings of randomly chosen bit sequences of length 161280) to calculate the respective BER values. Please note that these

<sup>4</sup>Dynamic detection algorithm assumes at least one 1-bit per code, which is the case for all RLIM <sub>$i$</sub> ( $n$ ) but not necessarily for Uncoded, ISI-free, and Hamming schemes. To address this issue for these coding schemes, we used a modified dynamic detection algorithm from [17], which introduces additional channel-specific parameters *min* and *spacing* alongside  $a$ . Through pilot signal transmissions for these schemes, we determined *min*, optimal  $a$ , and optimal *spacing* values.

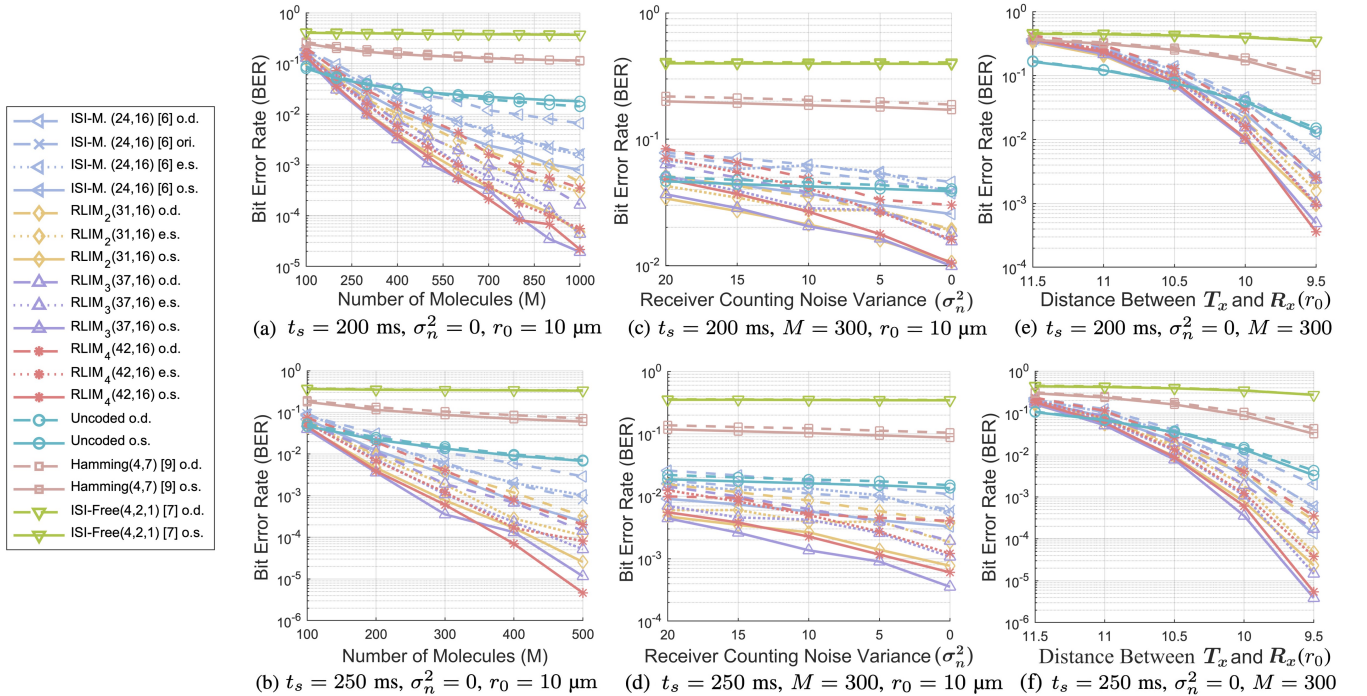


Fig. 5: MC Simulation Results for Different Parameters

specific number of bits have been chosen to ensure that all different block lengths of 4, 8, 12, and 16 perfectly divide these numbers, ensuring a fair comparison among coding methods in Fig. 4. Note that in Figs. 4 and 5,  $\text{RLIM}_1(n, k)$  is referred to as ISI-mitigating codes [6] of length  $n$  with block length  $k$  (i.e., ISI-M.  $(n, k)$ ), as they are equivalent.

## B. Evaluation of Simulation Results

1) *Impact of Block Length on Performance:* The simulation results for different block lengths  $k$  (i.e., different information sets  $\{0, 1\}^k$ ) are provided in Fig. 4(a) and (b). The corresponding values of  $\{x_i^k\}$ , whose derivations follow a similar process to those given in formulae 18-21, are shown in Table IV. Note that, in Figs. 4 and 5, o.d., ori., e.s., and o.s., stand for optimal dynamic, original<sup>1</sup>, estimated static, and optimal static respectively. These figures demonstrate that increasing the coding block length  $k$  generally enhances performance for higher-order RLIM codes, though it slightly reduces the performance of ISI-mitigating codes. Notably, in both Fig. 4(a) and (b), the best overall performance among all coding schemes and block lengths is achieved when a block length of 16 is used. This is why we chose  $k = 16$  for the remainder of comparisons. Note that the normalizations of molecule count and signal interval values for block lengths 4, 8, and 12 (not shown for brevity) follow the same process as for block length 16, as detailed in Tables I and II.

2) *Effects of Different Parameters:* As can be inferred from Fig. 5, higher molecule count and signal interval values improve BER, while higher  $r_0$  and receiver noise  $\sigma_n^2$  levels degrade it. Increasing the coding order  $i$  initially improves BER, but we conjecture that benefits diminish after a certain value of  $i$ , especially with shorter coding block lengths, as can be seen in Fig. 4(a) and (b). Additionally, at greater distances between  $T_x$  and  $R_x$  ( $r_0$ ), the performance of all coding methods (including Uncoded) degrades significantly, becoming unreliably worse. In such situations, the Uncoded method, however, surpasses all others, as shown in Fig. 5(e) and (f).

3) *Storage Requirements and Trade-offs:* While increasing the block length  $k$  can improve BER, it exponentially raises memory requirements, as each  $\text{RLIM}_i(n, k)$  requires  $n \cdot 2^k$  bits of storage space. These trade-offs must be carefully considered for practical applications of the proposed coding scheme. For  $k = 8, 12, 16$ , the proposed RLIM codes of order  $i \geq 2$  still outperform others (in their respective detection technique categories), as demonstrated in Fig. 4(a) and (b). Accordingly, if data storage capacity is limited, opting for  $k = 8$  or  $k = 12$  instead of  $k = 16$  is advisable. For future comparative simulations of our proposed family of codes, we recommend using a coding block length of at least 12 for a fair comparison, with  $k = 16$  being a more preferable option.

4) *Equivalence with Run-Length-Limited Codes for Drift-Excluded Channels:* For a non-drift channel, a key observation is that for all RLIM, the optimal static threshold detection method consistently outperforms the optimal dynamic threshold method. Consequently, dynamic threshold detection would only be necessary when the parameters of MC channel

fluctuates over time. Henceforth, it is no longer necessary to assume the presence of a single 1-bit in a code. Thus, for future uses with static threshold through a non-drift static channel, we make the enhancement in Eq. (23) for RLIM codes, making them equal to run-length-limited (RLL) codes of order  $(i, \infty)$  of length  $n$  [15]. Please note that implementing this enhancement would eliminate the need for Lines 6–16 in Algorithm 1.

$$\text{RLIM}_i(n) = \left[ \mathbf{0}_{|\mathcal{C}_i(n-i)|}^i \mid \mathcal{C}_i(n-i) \right] = \text{RLL}_n(i, \infty) \quad (23)$$

There is a thesis [22], where the authors applied the RLL codes to MC. However, as the authors did not incorporate the ordering  $(i, \infty)$  or use the RLIM error correction method outlined in Algorithm 2, they obtained numerical results in which RLL codes were surpassed by Uncoded in terms of BER.

## C. Time-Varying Drift Channel Model and Gains from Dynamic Threshold

In many real-world MC scenarios, the channel may exhibit random or time-varying drift, causing the arrival profiles of information molecules to fluctuate from one symbol interval to the next. Under such non-stationary conditions, a well-tuned dynamic threshold scheme can significantly outperform an optimal static threshold, since the latter fails to adapt to shifting channel conditions. To illustrate this advantage, we adopt a particle-tracking model, based on the simulator [23], that extends the discrete-time update formula given in Eq. 18.

At each simulation time step of duration  $\Delta t$ , the drift velocity  $\mathbf{v}(t)$  is updated according to the discrete-time approximation of an Ornstein–Uhlenbeck (OU) process with a nonzero mean:

$$\mathbf{v}(t + \Delta t) = \mathbf{v}(t) + \frac{1}{\tau_{\text{drift}}} \left( \mathbf{v}_{\text{mean}} - \mathbf{v}(t) \right) \Delta t + \sqrt{\frac{2\sigma_v^2 \Delta t}{\tau_{\text{drift}}}} \boldsymbol{\xi}(t), \quad (24)$$

where  $\tau_{\text{drift}}$  is the drift correlation timescale,  $\sigma_v^2$  governs the variability of the drift,  $\mathbf{v}_{\text{mean}}$  is the mean drift velocity, and  $\boldsymbol{\xi}(t)$  is a three-dimensional vector whose components are independently drawn from  $\mathcal{N}(0, 1)$ . The Ornstein–Uhlenbeck process is a classical stochastic model widely employed to capture fluctuating physical quantities in many natural and engineered systems (see, e.g., [24] and [25]). Once the drift velocity is updated via (24), each molecule’s position is updated by

$$\mathbf{r}(t + \Delta t) = \mathbf{r}(t) + \mathbf{v}(t + \Delta t) \Delta t + \Delta \mathbf{w}(t), \quad (25)$$

where  $\Delta \mathbf{w}(t)$  is a three-dimensional Gaussian random vector. Each component of  $\Delta \mathbf{w}(t)$  is drawn independently from  $\mathcal{N}(0, 2D \Delta t)$ , thereby modeling the diffusive displacement in accordance with Eq. 18.

We use the same simulation parameters from Table III. Table V further specifies the drift and particle-tracking parameters employed in our drift-included MC simulations. The settings in Table V produce a moderate but slowly varying drift that causes noticeable changes in the mean molecule arrival count over successive intervals. To prevent excessive compu-

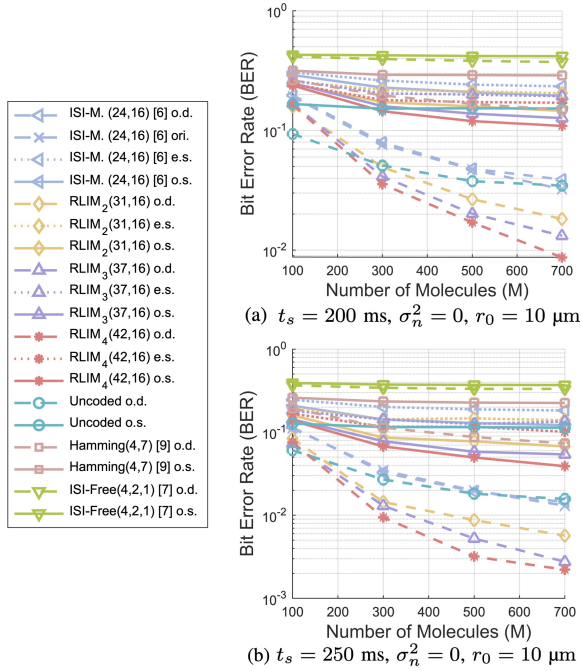


Fig. 6: MC Simulation Results with Time-Varying Drift

TABLE V: Drift and Particle-Tracking Parameters for Time-Varying MC Simulations

Parameter	Value
Time step ( $\Delta t$ )	1 ms
Drift correlation timescale ( $\tau_{\text{drift}}$ )	10 s
Drift standard deviation ( $\sigma_v$ )	10 $\mu\text{m/s}$
Mean drift velocity ( $\mathbf{v}_{\text{mean}}$ )	[1, 0, 0] $\mu\text{m/s}$
Max molecule age	5 s
Emitter (Tx) location	[0, 0, 0] $\mu\text{m}$
Receiver (Rx) center	[ $r_0$ , 0, 0] $\mu\text{m}$

tational overload, the channel capacity is set to 5 seconds. For a signal interval of 0.2 seconds, this corresponds to a channel memory of 25 in the Uncoded case.

The corresponding BER values of compared coding schemes for a generic MC channel with a time-varying drift is provided in Fig. 6. Under these non-stationary conditions, a dynamic threshold consistently achieves lower bit error rates<sup>5</sup> than the corresponding fixed threshold-based method, demonstrating the need for adaptive detection in such MC channels. This requirement justifies the inclusion of at least one 1-bit in each RLIM-coded symbol, distinguishing RLIM from conventional run-length-limited codes and enabling the use of dynamic detection. As can be seen in Fig. 6, RLIM codes with dynamic detection surpasses the compared methods.

#### IV. CONCLUSIONS

This paper presents a novel infinite family of codebooks,  $\text{RLIM}_i(n)$ , which we have developed to enhance molecular

<sup>5</sup>For particle-tracking simulations, to determine the optimal detection parameters, we initially sent a total of 61440 bits (8 contiguous runs of the encodings of randomly chosen bit sequences of length 7680). After having determined the optimal detection parameters, to calculate each respective BER value, we then sent a total of 128000 bits (8 contiguous runs of the encodings of randomly chosen bit sequences of length 16000).

communication channel performance through improved error correction capabilities while maintaining simplicity. We have demonstrated that these codes achieve a substantial bit error rate (BER) improvement over compared coding schemes particularly when  $i \in \{2, 3, 4\}$ . The key feature of  $\text{RLIM}_i(n)$  is that each 1-bit is followed by at least  $i$  0-bits.

Simulation results indicate that, under generic zero-drift conditions, the requirement for each  $\text{RLIM}_i(n)$  code to include at least one 1-bit is unnecessary. In fact, removing this constraint makes the  $\text{RLIM}_i(n)$  codebook equal to a run-length-limited (RLL) code of order  $(i, \infty)$ . Nevertheless, the practical  $\text{RLIM}_i(n, k)$  encoding scheme, which is a subset of  $\text{RLIM}_i(n)$  with cardinality  $|\text{RLIM}_i(n, k)| = 2^k$ , retains its unique power constraint and specialized error correction algorithm. Conversely, when drift is present and time-varying, the 1-bit constraint is no longer redundant, and our findings confirm its importance for robust performance under such channel conditions.

Future work should focus on developing more precise theoretical distributions for  $iN_0^{\text{average}}$  and  $iN_1^{\text{average}}$ , which could improve the BER of static threshold estimation and potentially eliminate the necessity of sending pilot signals before communication. Overall, the success of the proposed  $\text{RLIM}_i(n)$  and  $\text{RLIM}_i(n, k)$  codes represents a significant advancement in MC channel coding.

#### ACKNOWLEDGMENT

Melih Şahin, the first author, dedicates this work to his late grandfather Muzaffer Şahin, whose battle with cancer motivated him to pursue research in Molecular Communication. This work is driven by the belief that advancements in this field can pave the way for more effective cancer treatments.

#### CODE AVAILABILITY

Python implementations of binomial simulator, code space generation, encoding, decoding, analytical threshold estimation, detection, and error correction algorithms for any chosen  $\text{RLIM}_i(n, k)$  are provided in the following code repository: <https://github.com/MelihSahinEdu/McChannelCoding.git>

#### REFERENCES

- [1] M. Kusu, E. Dinc, B. A. Bilgin, H. Ramezani, and O. B. Akan, "Transmitter and receiver architectures for molecular communications: A survey on physical design with modulation, coding, and detection techniques," *Proceedings of the IEEE*, vol. 107, no. 7, pp. 1302–1341, 2019.
- [2] D. Malak and O. B. Akan, "Molecular communication nanonetworks inside human body," *Nano Communication Networks*, vol. 3, no. 1, pp. 19–35, 2012.
- [3] O. B. Akan, H. Ramezani, T. Khan, N. A. Abbasi, and M. Kusu, "Fundamentals of molecular information and communication science," *Proceedings of the IEEE*, vol. 105, no. 2, pp. 306–318, 2017.
- [4] T. Nakano, A. W. Eckford, and T. Haraguchi, *Molecular Communication*. Cambridge University Press, 2013.
- [5] D. Kilinc and O. B. Akan, "Receiver design for molecular communication," *IEEE Journal on Selected Areas in Communications*, vol. 31, no. 12, pp. 705–714, 2013.
- [6] A. O. Kislal, B. C. Akdeniz, C. Lee, A. E. Pusane, T. Tugcu, and C.-B. Chae, "Isi-mitigating channel codes for molecular communication via diffusion," *IEEE Access*, vol. 8, pp. 24 588–24 599, 2020.

- [7] P.-J. Shih, C. Han Lee, P.-C. Yeh, and K.-C. Chen, "Channel codes for reliability enhancement in molecular communication," *IEEE Journal on Selected Areas in Communications*, vol. 31, pp. 857–867, 2013.
- [8] M. Kuran, H. B. Yilmaz, T. Tugcu, and I. Akyildiz, "Modulation techniques for communication via diffusion in nanonetworks," 12 2013.
- [9] R. W. Hamming, "Error detecting and error correcting codes," *The Bell System Technical Journal*, vol. 29, no. 2, pp. 147–160, 1950.
- [10] Y. Lu, M. D. Higgins, and M. S. Leeson, "Diffusion based molecular communications system enhancement using high order hamming codes," in *2014 9th International Symposium on Communication Systems, Networks & Digital Sign (CSNDSP)*, 2014, pp. 438–442.
- [11] M. Şahin, <https://BioRender.com/p99d576>, 2024, created in BioRender.
- [12] E. B. Pehlivanoglu, B. D. Unluturk, and O. B. Akan, *Modulation in Molecular Communications: A Look on Methodologies*. Cham: Springer International Publishing, 2017, pp. 79–97.
- [13] H. B. Yilmaz, A. C. Heren, T. Tugcu, and C.-B. Chae, "Three-dimensional channel characteristics for molecular communications with an absorbing receiver," *IEEE Communications Letters*, vol. 18, no. 6, pp. 929–932, 2014.
- [14] H. B. Yilmaz, C.-B. Chae, B. Tepekule, and A. E. Pusane, "Arrival modeling and error analysis for molecular communication via diffusion with drift," in *Proceedings of the Second Annual International Conference on Nanoscale Computing and Communication*, ser. NANOCOM' 15. New York, NY, USA: Association for Computing Machinery, 2015.
- [15] B. Marcus, R. Roth, and P. Siegel, *Introduction to Coding for Constrained Systems*, 2001. [Online]. Available: <https://personal.math.ubc.ca/~marcus/Handbook/>
- [16] D. Tang and L. Bahl, "Block codes for a class of constrained noiseless channels," *Information and Control*, vol. 17, no. 5, pp. 436–461, 1970.
- [17] M. Şahin, B. E. Ortlek, and O. B. Akan, "Molecular arithmetic coding (moac) and optimized molecular prefix coding (mopc) for diffusion-based molecular communication," *IEEE Transactions on Molecular, Biological, and Multi-Scale Communications*, vol. 11, no. 1, pp. 66–77, 2025.
- [18] N. Garralda, I. Llatser, A. Cabellos-Aparicio, and M. Pierobon, "Simulation-based evaluation of the diffusion-based physical channel in molecular nanonetworks," in *2011 IEEE Conference on Computer Communications Workshops (INFOCOM WKSHPS)*, 2011, pp. 443–448.
- [19] M. J. Saxton, *Modeling 2D and 3D Diffusion*. Totowa, NJ: Humana Press, 2007, pp. 295–321.
- [20] M. C. Gursoy, E. Basar, A. E. Pusane, and T. Tugcu, "Index modulation for molecular communication via diffusion systems," *IEEE Transactions on Communications*, vol. 67, no. 5, pp. 3337–3350, 2019.
- [21] B. Tepekule, A. E. Pusane, H. B. Yilmaz, C.-B. Chae, and T. Tugcu, "Isi mitigation techniques in molecular communication," *IEEE Transactions on Molecular, Biological and Multi-Scale Communications*, vol. 1, no. 2, pp. 202–216, 2015.
- [22] M. Damrath, "Channel coding in molecular communication," 2020, online. [Online]. Available: <https://nbn-resolving.org/urn:nbn:de:gbv:8-mods-2020-00366-4>
- [23] H. B. Yilmaz, "Molecular communication (mucin) simulator matlab central file exchange. 2020." [Online]. Available: <https://www.mathworks.com/matlabcentral/fileexchange/46066-molecular-communication-mucin-simulator>
- [24] C. Gardiner, *Stochastic Methods: A Handbook for the Natural and Social Sciences*, 4th ed., ser. Springer Series in Synergetics. Springer Berlin, Heidelberg, Jan.16 2009, hardcover, XVIII, 447 pages. Copyright Springer-Verlag Berlin Heidelberg 2009.
- [25] N. V. Kampen, "Stochastic processes in physics and chemistry," ser. North-Holland Personal Library, N. V. Kampen, Ed. Amsterdam: Elsevier, 2007.



**Melih Şahin (Student Member, IEEE)** graduated from both Ankara Science High School and Bilsen in 2019. He started studying a B.Sc. degree in School of Computing at Korea Advanced Institute of Science and Technology (KAIST) in 2020, completing first year of his degree in 2021. He then transferred to Koç University, Türkiye, where he graduated with a B.Sc. degree in Computer Engineering, together with a minor in Mathematics and a track on AI in June 2024. He is currently pursuing a MSc. degree in Electrical and Electronics Engineering at Koç

University. He holds many prestigious international and national awards in scientific research and painting. His most notable achievements include a 4<sup>th</sup> place Grand Award in Mathematics at Intel International Science and Engineering Fair (ISEF) 2018 Pittsburgh, as well as a global bronze medal (3<sup>rd</sup> place) at Toyota International My Dream Car Art Contest 2013 in the age category of 10-12. His current research interests are Coding Theory, Molecular Communication, Quantum Computing, Computation Theory, Machine Learning, and Algebraic Combinatorics.



**Ozgur B. Akan (Fellow, IEEE)** received the PhD from the School of Electrical and Computer Engineering Georgia Institute of Technology Atlanta, in 2004. He is currently the Head of Internet of Everything (IoE) Group, with the Department of Engineering, University of Cambridge, UK and the Director of Centre for neXt-generation Communications (CXC), Koç University, Türkiye. His research interests include wireless, nano, and molecular communications and Internet of Everything.